Energy- and Safety-Aware Operation of Battery-Powered Autonomous Robots in Agriculture

Shashank Dhananjay Vyas, Vigneshwar Kumutha Subash, Manav Mepani, Sai Venkatesh, Arpita Sinha, Anirban Guha, and Satadru Dey

[1] ***Abstract*—To improve food security and environmental sustainability amid the global crisis of climate change and nutrition quality requirements as well as low cost agricultural needs and electricity issues, particularly in developing countries like India, it is essential to combine autonomy and newer energy storage methods with traditional agriculture. Existing field robotic mechanisms, path planning methods and battery energy management systems are designed independent of each other. To ensure energy efficient and safety aware operation of autonomous agricultural robots, coordination between aforementioned techniques is necessary. With the aim to provide such solution, in this work we propose a framework to integrate robot mechanism, path planning and battery management system. Simulations are performed to validate the performance of the algorithm.**

***Index Terms*—Agriculture, Autonomous Robots, Path Planning, Batteries.**

I. Introduction

A smart agriculture architecture incorporating portable hardware can alleviate many of the bottlenecks to food accessibility [1], [2]. In this paper, we propose a multidisciplinary framework for energy and safety aware operation of battery powered autonomous robot in agriculture. There are numerous instances of large mobile agricultural machinery, mostly crop harvesters, both in literature [3] as well as in the commercial domain [4], [5]. However, a design suitable for the small and fragmented farms seen in large parts of the developing world, is not available. Whether scaling down the existing large harvester design needs other structural changes is an open question. Specifically, though quite a few designs exist for onion harvesting [3], [6]–[12], a design suitable for a small and unstructured farm is not available. LePori and Hobgood [6] have explored a design in which the harvested onions are reversed as they are conveyed up an inclined conveyor, making it easy for the plants to be separated from the onions. The design proposed by Hiroshi [7] which combines digging, lifting, conveying, topping and separating in a single machine, seems to have inspired many of the later designs. The design given by Nisha and Sridhar [10] is the most simple of these and is perhaps suitable for a relatively small harvester. However, choosing one suitable for the small machine is not trivial. Moreover, a small autonomous mobile agricultural machine/harvester has not even been theoretically investigated so far. Designing one would require a model for predicting the traction and subsequent power requirement, a battery model for predicting the energy status and a path planning algorithm for guiding the rover, all integrated in a single simulation environment. This is an unexplored field to the best of our knowledge.

The applications of path planning in agriculture are diverse and cover various topics and scenarios. Extensive studies of ground agricultural robot are available in [13] and [14], while [15] surveys the robotic harvester systems and [16] surveys the uses of drone in agriculture. The applications of path planning are found in various agricultural settings, including vineyards [17], orchards [18], greenhouses [19], and paddy farms [20]. The use cases for path planning encompass tasks such as navigation, monitoring, targeted spraying, and harvesting. Some studies propose specific path planning algorithms tailored to agricultural environments (see [14] and references within) and machinery, while others focus on general-purpose path planning algorithms applicable to agriculture. Vision-based navigation and guidance for robotic vehicles is studied in [21] while the authors in [22] studies path tracking problem for autonomous harvesting. The work presented in this paper complements the studies done in [23] where the stereo vision and deep learning techniques are used to identify the crop rows and determines the navigation waypoints that the harvester should follow.

Most of the battery energy management research is focussed on applications such as passenger automotive vehicles and renewable energy storage. These existing solutions cannot be directly transferred to the applications of battery powered robots in fields due to various factors such as dissimilar power consumption profiles leading to different energy and safety conditions, planning priorities for task completion and locomotion based on robot size and shape. Some works in the past have tried to address this issue. For example, battery charge scheduling for longer life robots under uncertainties has been explored in [24]. In [25], [26] and [27], charge estimation approaches such as Kalman filters and H_∞ observers were explored for mobile robots. The work [28] explored energy estimate models to be used for mobile robot autonomy. In [29], autonomous battery management has been explored for mobile robots. These approaches are limited in the sense that

S. D. Vyas and S. Dey are with the Department of Mechanical Engineering, The Pennsylvania State University, University Park, PA 16802, USA (e-mail: {sbv5192, skd5685}@psu.edu).

V. K. Subash, M. Mepani, S. Venkatesh, A. Sinha, and A. Guha are with IIT Bombay, India (e-mail: vigneshwarsk@gmail.com, mepanimanav@gmail.com, saivenkatb20@gmail.com, anirbanguha1@gmail.com, arpita.sinha@iitb.ac.in).

[1]This work was supported in part, by the National Science Foundation (NSF) under Grant No. 2050315 and the Technology Innovation Hub for IoT and IoE, IIT Bombay, under NSF's DCL 22-040 for United States-India collaborative research initiative. The opinions, findings, and conclusions or recommendations expressed are those of the author(s) and do not necessarily reflect the views of the National Science Foundation.

they do not fully capture internal battery physics. These results in incomplete understanding of internal battery states which are highly essential for energy and safety aware operation of autonomous field robots. Hence, we utilize the Single Particle Model (SPM) which is a physics-based battery model to capture the battery internal states. We provide an estimate on the battery instantaneous energy and raise an alarm indicating whether a fault has occurred resulting in energy and safety aware operation.

Traditionally, for battery-powered autonomous robots, robotic mechanism do not consider battery and path planning constraints while conventional battery management does not take into account robot mechanism and path planning constraints. For increased energy efficiency and safety, coordinated efforts of robot mechanism design, path planning and battery management are required. Only few works in the literature have briefly mentioned this issue. For example, an intelligent power management considering remaining battery capacity was explored in [30]. In [31], remaining energy estimation was used to intelligent allocate tasks to mobile robots. Although these studies show the promise, a comprehensive solution framework still remains an open problem.

In light of the aforementioned research gaps, we propose an integrated framework of robot mechanism design, path planning and battery management for energy and safety aware operation of battery powered autonomous agricultural robots. Essentially, the main contribution of this paper is an algorithmic architecture which enables iterative interaction between different components of the overall mechanism to ensure energy efficient and safe locomotion of the robots. The rest of the paper is organized as follows. In Section II, we start with a brief overview of our battery powered robot autonomy architecture, operation and algorithm. Then we proceed to describe the robot mechanism design, battery model and estimation, and path planning algorithms in detail. In Section III, we discuss the results obtained from the simulations. Finally, Section IV concludes the paper.

II. GENERAL FRAMEWORK FOR ENERGY- AND SAFETY-AWARE ROBOT OPERATION

A schematic of the proposed algorithmic framework is shown in Fig. 1. As shown in the figure, a battery-powered robot performs the locomotion and an agricultural task. In this paper, the robot is an onion harvester and the agricultural task is harvesting onions in an onion-field. The robot includes a proportional-integral type controller which receives reference position and velocity trajectories from the path planning algorithm, and in turn commands appropriate force for the robot to move. Accordingly, the robot moves around the onion-field and continue performing the harvesting task. In the mean time, battery system is monitored continuously to track battery energy and any potential fault occurrences. Once the battery energy is depleted to a level such that only energy left is just enough for return, the robot returns to the base. Furthermore, even if there is enough battery energy left for harvesting, but there is a battery fault – the robot returns to base for safe handing of the battery. In the next subsections, we will discuss various elements of this framework.

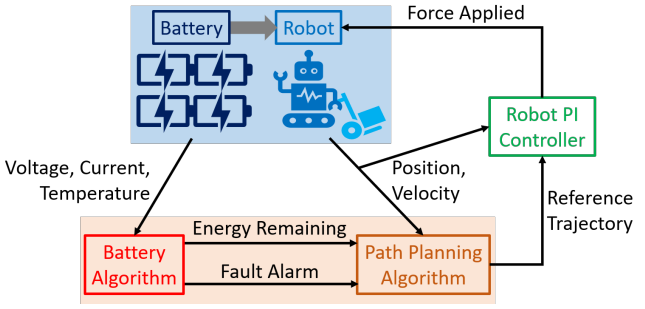

Fig. 1. Schematic of the proposed algorithmic framework.

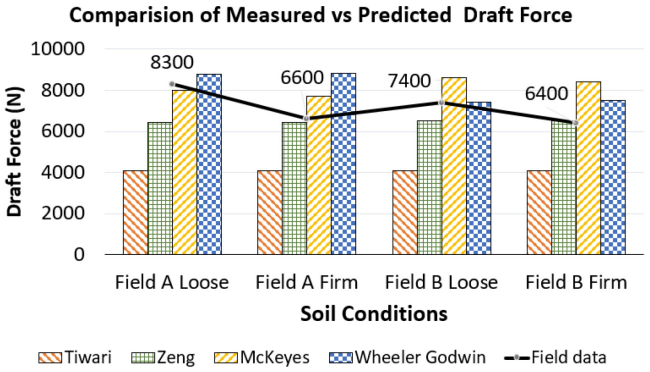

Fig. 2. Choosing appropriate model for predicting harvesting force.

A. Robot Mechanism Design

In order to design an onion harvester, it is necessary to develop a model for predicting the power required to drive the harvester, both while it is harvesting and while it is moving on the soft soil but is not harvesting. A review of literature in this domain shows modelling attempts ranging from fundamental (first-principle) to empirical. The general trend has been to model the force required for digging and force of traction separately. To choose a suitable model for the former, we analyzed the analytical model developed by Zeng et al [32], the semi-empirical models of McKyes and Ali [33] and Wheeler and Godwin [34] the empirical model of Tiwari [35]. The predictions of these models on the test conditions described by Tong et al [36], when compared with the test results given by Tong et al [36] (Fig. 2), allowed us to choose the model of Zeng et al. [32]. This was used for estimating the power required for the operation which led to appropriate motor and battery sizing. For evaluating various terms in the equations developed by Zeng et al [32], some assumptions had to be made about the harvester. From a detailed CAD model (Fig. 3), the weight was estimated to be 50 kg. The speed was considered to be 1 m/s while harvesting and 2 m/s while transporting. From the onion cultivation data reported by Khura [37], the maximum depth to which a plough would need to dig into the soil for harvesting would be 70 cm and mean depth would be 35 cm. In this work, we considered a harvesting depth of 40 cm. A schematic diagram of the harvester is shown in Fig. 4.

Fig. 3. Detailed CAD model of the harvester.

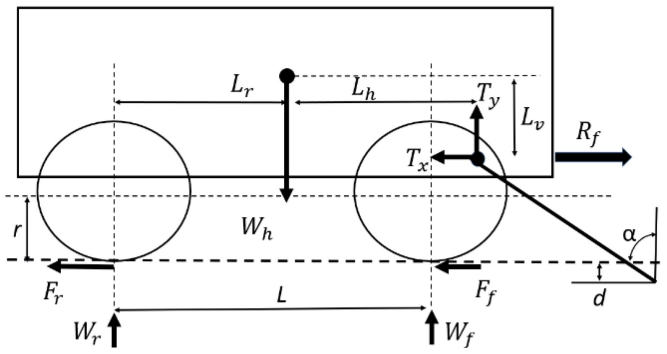

Fig. 4. A schematic diagram of the harvester.

The following equations from the model of Zeng et al [32] were used to calculate the force required for digging: $T_x = -F_{blade}\sin\alpha + P_p\cos\cos(\alpha-\delta) + F_{side}\cos\beta + \frac{W_b a_h}{g}$ and $T_y = F_{blade}\cos\alpha + P_p\sin\sin(\alpha-\delta) + F_{side}\sin\beta + \frac{W_b a_v}{g}$, where P_p is force due to passive earth pressure, a_v is acceleration in vertical direction, F_{side} is side friction force, β is side friction angle, δ is friction angle between soil and blade, and W_b is weight of blade Zeng et al considered F_{blade} to be negligible since the frictional resistance and cohesion of soil was small. For our application, though the contribution is somewhat small, it was included as: $F_{blade} = \frac{c_a W d}{\cos\alpha}$ where W is the width of the blade, d is the vertical distance of the tip of the blade from the soil surface, and α is the acute angle between blade and soil surface, and c_a soil tool adhesion. For calculating the length of failure wedge, assuming it to be of crescent type, the equations used by McKyes and Ali [33] was used as follows: $L_W = (\tan\tan\alpha + \cot\cot\alpha_p)d$ where α_p is the inclination angle of soil failure wedge. Solving these two equations would give us the total digging force required.

The equations for the tractive force were as follows:

$$W_h - T_y - W_r - W_f = 0, R_f - F_r - F_f - T_x = 0, \quad (1)$$

$$W_r L_r - W_f(L - L_r) - T_x L_v - T_y L_h - F_f r' - F_r r' + R_f L_v = 0, \quad (2)$$

Here the parameters L, L_r, L_h, W_h and r are known, and can be obtained from the CAD model. The parameters d and α are defined as inputs. T_x and T_y were obtained by solving the model of Zeng et al. The rest of the force variables R_f, W_f, W_r, F_r and F_f are unknown. Since there were five unknown variables and only three equations, we used equations given by Brixius [38] to formulate more equations to solve for these variables. Knowing certain parameters of the tire and soil conditions like the cone index (CI) and tire cross sectional dimensions (width b and height h), tire diameter d', tire deflection δ' and observed slip, the Brixius mobility number (B_{nf}, B_{nr}) can be calculated and from that, the motion resistance of the wheels can be found using equations (3). Here the slip (S) was calculated as the average slip observed while moving the vehicle for 2 m distance and counting the revolution of the wheels. The cone index was taken as 150 based on field observation and comparing it with the information available on research papers for the soil condition expected in our case.

$$B_{nf} = \frac{CIbd'}{W_f}\frac{1+5\frac{\delta'}{h}}{1+3\frac{b}{d'}}, B_{nr} = \frac{CIbd'}{W_r}\frac{1+5\frac{\delta'}{h}}{1+3\frac{b}{d'}}, \quad (3)$$

$$\frac{F_u}{W_u} = \frac{1}{B_{nu}} + 0.04 + \frac{0.5S}{\sqrt{B_{nu}}}, \quad u \in \{f, r\} \quad (4)$$

Equations (1), (2), (3) and (4) are now solved to obtain R_f, W_f, W_r, F_r and F_f. For validating these models, we built a mini prototype of the harvester with just the frame and blades. We utilized a S type 200 kg load cell in combination with HX711 A/C converter, Micro SD reader and Arduino Uno for measuring the total pull force required for various conditions like, (i) Transporting the harvester in the field, and (ii) Transporting and digging at different rake angles. The average loads from 4 trials for moving with digging and 3 trials for moving without digging were 186.9 N and 24.7 N respectively. The corresponding values predicted by our model were 200.7 N and 30.3 N. The reasonable agreement between the values predicted by our model and the experimentally determined values gave us confidence to use this model for further studies.

Solving all the equations for the tractive force requires iterative equation solving techniques. It was envisaged that it would be difficult to implement such a model in conjunction with additional iterative procedures needed for the path planning controller and the battery model based energy predictor. To simplify the process and avoid solving the harvester modelling equations repeatedly, we looked at the major contributors to the pull force required and identified that for a particular field with specific operational parameters being set, it is possible to consider only the speed and mass of the harvester as variables. Hence, the equations were solved repeatedly only once for the purpose of generating a database from which the following regression equations were formulated for predicting the tractive forces: *Torque required for moving and harvesting* = $-0.00003t^2 + 0.0563t + 0.4881$, and *Torque required for moving without harvesting* = $-0.00003t^2 + 0.0444t - 0.2743$. In this exercise, we assumed the average mass of an onion to be 52 g (as reported by Khura [1]), a speed of 1 m/s while harvesting and 2 m/s while moving without harvesting.

B. Battery Models and Algorithms

Here, we discuss the battery model and the battery energy estimation and fault alarm signaling algorithm.

1) Electrochemical and Thermal Models: First, we discuss the electrochemical part of the battery model. We have used the SPM framework in our model where the electrodes are

approximated as spherical particles. Particularly we adopted the anode dynamics from SPM in our work [39], [40], which the captures the spatio-temporal Lithium concentration in anode $c_a(r,t)$ (unit mol/m^3, with radial direction r and time t) as follows:

$$\frac{\partial c_a(r,t)}{\partial t} = \frac{D}{r^2}\frac{\partial}{\partial r}\left(r^2\frac{\partial c_a(r,t)}{\partial x}\right), \tag{5}$$

$$\left.\frac{\partial c_a(r,t)}{\partial r}\right|_{r=0} = 0, \quad \left.\frac{\partial c_a(r,t)}{\partial r}\right|_{r=r_0} = -\eta I(t), \tag{6}$$

where D is the diffusion coefficient in m^{2}s^{-1}, r_0 is the particle radius in m, I is the battery current, $\eta = 1/a_a F D v_a$ with v_a is the anode volume in m^3, a_a is the specific surface area in m^{-1}, and F is the Faraday's constant in Cmol^{-1}. The dynamics for the battery terminal voltage is given by [39], [41]: $V_e(t) = U(c_a(0)) - R_i I(t) - g(I(t))$, where V_e is the terminal voltage, $U(c_a(0))$ captures the open circuit potential, R_i captures the Ohmic resistances effects, and $g(I(t))$ captures a nonlinear resistance-like term arising from Butler-Volmer kinetics.

Next, the thermal dynamics is adopted from [42], [43], and given as follows:

$$mC_p\frac{\partial T}{\partial t} = hA(T - T_{en}) + I(U(c_a(0)) - V_e), \tag{7}$$

where T is battery temperature, m is the mass, C_p in J(kgK)$^{-1}$ is the specific heat capacity of the cell, h is the convection heat transfer coefficient between the cell surface and the environment, T_{en} is the environmental temperature, and $I(U(c_a(0)) - V_e$ i)s the heat generation. Under a thermal fault, the heat generation will be changed to $I(U(c_a(0)) - V_e) + \theta_T$ where θ_T is the abnormal heat generation due to the fault [44].

2) Energy Estimation and Fault Alarm Signal: Energy estimation and fault alarm generation are performed by model-based observer methods. We use the approaches presented in [44], for designing the voltage and temperature observers. Following [44], we first convert the Partial Differential Equation (PDE) model (5)-(6) into an approximated Ordinary Differential Equation (ODE) model by using finite difference discretization method. Subsequently, we design a state observer of the form given below:

$$\dot{\hat{c}}_1 = A_n\hat{c_1} + B_n I(t) + K_1(V(t) - \hat{V}(t)), \tag{8}$$

$$\hat{V}_e(t) = U(\hat{c}_1) - R_i I(t) - g(I(t)), \tag{9}$$

where $\hat{c_1}$ and $\hat{V}_e$ are the estimates of the concentration c_a and voltage V_e, respectively, A_n and B_n are matrices derived from finite difference approximation, K_1 is the observer gain that amplifies the correction error term $V(t) - \hat{V}(t)$. This in turn is used to estimate the energy as follows: $\hat{E}_b(t) = \hat{V}_e(t)I(t)$, $E_r(t) = E_{max} - \hat{E}_b(t)$, where E_r is energy remaining, E_{max} is maximum battery energy, and $\hat{E}_b(t)$ is the energy consumed by the battery till the time t. Similarly, we use the following temperature observer to generate the fault alarm.

$$mC_p\frac{\partial \hat{T}}{\partial t} = hA(\hat{T} - T_{en}) + I(U(\hat{c}_1 - V_e) + K_2(T - \hat{T}), \tag{10}$$

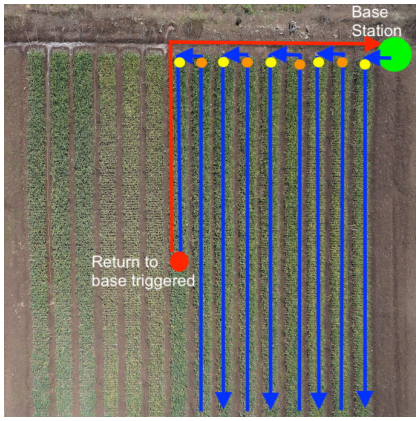

Fig. 5. Path of the harvester robot on an onion field.

where $\hat{T}$ is the estimated temperature and K_2 is the observer gain. Based on the temperature estimation, temperature residual is obtained as $T_r(t) = T(t) - \hat{T}(t)$. We use following logic for fault alarm generation: if residual $|T_r| > r_{th}$ raise the alarm, i.e., $f = 1$, otherwise no alarm, i.e. $f = 0$, where r_{th} is a pre-defined threshold. The battery energy estimation and fault alarm signalling procedure is summarized in Algorithm 1. The algorithm takes in the measured values of voltage V_e, current I and temperature T as input, and outputs the values of $\hat{E}_b$ and f which are the energy remaining and the fault alarm, respectively.

Algorithm 1: Energy remaining and fault alarm signal

Input: Voltage V, Current I, Temperature T.
Output: Energy Remaining E_r, Fault Alarm f.

```
Using I in (9), obtain V̂_e.
Using V̂_e from step 1 and I, obtain E_r.
Using T, obtain T̂ from (10).
Using T̂ from step 4 and T, obtain T_r.
if |T_r| > r_th then
    Display "Fault Occurred".
    Return "Energy Remaining = E_r, Alarm f = 1".
else
    Display "No Fault".
    Return "Energy Remaining = E_r, Alarm f = 0".
end
```

C. Path-planning and autonomous navigation

Here, we discuss the path-planning technique for the autonomous navigation of the harvesting robot. The onion fields typically have rows of long, raised beds of onions, 1-1.5ft in width, with narrow passages between them. There are no obstacles on the field. The path of the robot follows the rows of onion as in Figure 5. The challenge is to decide the optimal condition when the robot should return to the base for recharging.

We are considering a base station next to the field for the robotic system. The robot starts and returns to the base station. The conditions under which the robot returns to the

base are (a) to unload the harvest when it exceeds its carrying capability, (b) if it needs battery recharging (c) if there is a fault in the battery. We assume the following: **[A1]** The robot knows the layout of the onion field. **[A2]** The robot moves at a constant speed. **[A3]** The robot localizes using GPS. **[A4]** The robot can align appropriately with the rows of onion plants for harvesting.

Algorithm 2: Energy Aware Path Planning

```
1  Input: energy_remaining, energy_required,
     return_to_base, fault_alarm, weight_of_harvest
2  Output: robot_position
3  if return_to_base is False
4        if energy_required is more than energy_remaining
5              return_to_base is True
6        end
7  end
8  if return_to_base is False or fault_alarm is Off or
     weight_of_harvest is within limits
9        new_robot_position = harvest_mode(current
     robot_position)
10 else
11       new_robot_position = return_mode(current
     robot_position)
12 end
```

At each time step, we calculate the energy the robot will need to reach the base station. If this energy is less than what is remaining in the battery, the robot can continue to harvest. However, when the energy is about to exceed the energy in the battery, the robot stops harvesting and returns to the base.

Algorithm 3: Harvest Mode

```
1  Input: current robot_position, field_layout
2  Output: new robot_position
3  if end of row reached
4        move to the next row
5  else
6        move forward
7  end
```

We present the path planning strategy in the Algorithms 2, 3, and 4. We first describe Algorithm 3 and 4. There are two modes for the robot - harvesting (Algorithm 3) and return to base (Algorithm 4). In the harvesting mode, the robot moves along a row (line 4 of Algo 3), and once the end of the row is reached, it turns and moves to the next row (line 6 of Algo 3) in a rusted scan pattern. We denote the point where the robot starts a row as the start-point of the row and similarly where it ends as the end-point (refer to Figure 5). In return to base mode, the robot first moves back to the start point of the row it is in (line 6 of Algo 4) and then moves along the periphery of the field to reach the base station (line 4 of Algo 4). The robot can calculate the distance to the base, which is required in Algo. 2 to find the energy required. The energy required is equal to the distance times force. Algorithm 2 checks the mode

Fig. 6. Onion-bed detection using OpenCV. The picture illustrates the onion plant during its initial growth phase, which appears less dense when contrasted with the period of harvest. However, the bed remains the same.

in which the robot needs to operate. Once the return to base is triggered, the robot does not go back to harvesting mode. During the harvesting mode, three conditions are checked for returning to base in line 8. If any of them are true, line 9 is executed else, line 11 is executed.

Algorithm 4: Return Mode

```
1  Input: current robot_position, field_layout,
     base_station
2  Output: new robot_position
3  if at the start of the row
4        move straight to the base station
5  else
6        move towards the start of the row
7  end
```

The Assumption A4 can be handled using a camera with on-board image processing capabilities. We can use image segmentation and contour detection to identify the onion bed as shown in Fig. 6. If the robot is not properly aligned, issuing a re-orientation command can ensure that the robot is aligned correctly. A detailed image processing method for onion-bed detection is available in [23].

III. RESULTS AND DISCUSSIONS

Here, we discuss simulation case studies. The robot model parameters were identified as discussed in Section II.A, and the battery and path planning algorithms were developed as discussed in Sections II.B and II.C, respectively. Battery parameters were taken from [44] and battery was assumed to have a parallel configuration of 58 cells. The framework was implemented in MATLAB R2022b environment. Specifically, we will discuss two cases: one under no-fault scenario when the robot returns as the battery is depleted, and the second case is under faulty scenario when the robot returns as there is a battery thermal fault.

A. Case Study 1

In this study, we create a nominal or no-fault scenario. The robot navigates the onion-field harvesting onions and returns when the battery is depleted. The robot trajectory under $X - Y$ coordinates is shown in Fig. 7(a) where the "blue" part represents moving and harvesting whereas the "red" part indicates returning. The velocity trajectory is shown

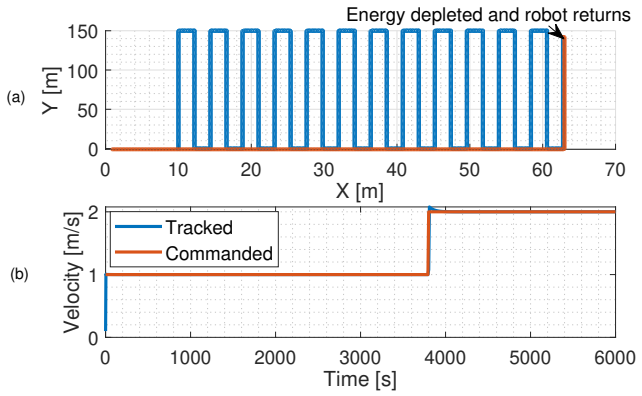

Fig. 7. (a) Trajectory of the robot under nominal scenarios and (b) velocity of the robot under nominal scenarios.

in Fig. 7(b) with "red" indicating commanded velocity by the path planning algorithm and "blue" indicating actual velocity tracking by robot proportional-integral control. The closeness of the commanded and actual tracking velocity verifies that the robot control performed reasonably well. The moving and harvesting were performed under 1 m/s velocity until approximately at 4712 s the battery energy was depleted to a level such that only energy left is just enough for return. Subsequently, the robot starts its return to the base with 2 m/s velocity. The battery parameters for a single cell are shown in Fig. 8. As can be seen from the top subplot of the figure, battery current is different under moving and harvesting part until 4712 s and changed to a higher current after that due to return. This is justified as the velocity changed from 1 to 2 m/s at 4712 s requiring more power from the battery. Furthermore, during the harvesting phase, it can be noted that battery current is increasing with respect to time reflecting the increase in mass as onions are collected. Corresponding battery voltage and temperature profiles are shown in bottom subplots of Fig. 8. Both of these subplots show the actual variables in "blue" and estimated variables in "red". Both of these estimates started from an incorrect initial condition and quickly converged to the actual values – which verifies that the battery estimation algorithms performed reasonably well. Furthermore, throughout the operation, the closeness of estimated and actual temperature verifies that the temperature residual does not cross the threshold – determining there is no fault.

B. Case Study 2

In this study, we consider a case when a battery thermal fault occurs during the operation. In the beginning, the robot starts moving and harvesting onions as shown in the $X-Y$ coordinates in Fig. 9(a). The "blue" line indicates the normal operation until the fault occurrence. In the battery simulation, we have injected a battery thermal fault around 4500 s, which leads to battery heat generation increase from $0.052W$ to $1.124W$. Accordingly, battery algorithm raises an alarm and the robot returns to the base, as shown in "red" part of the trajectory in Fig. 9(a). Corresponding velocity is shown in Fig. 9(b) where moving and harvesting velocity of 1 m/s is changed to return velocity of 2 m/s after the fault occurrence

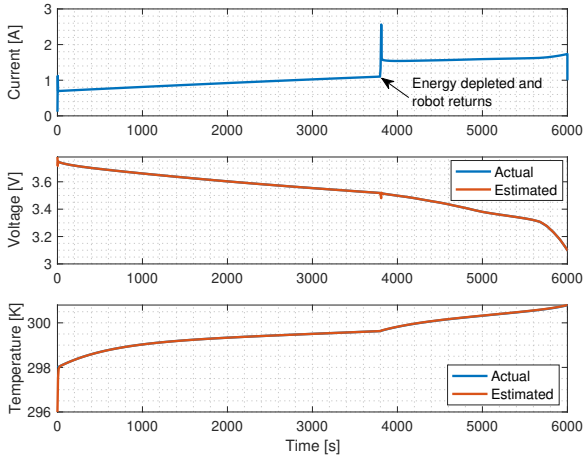

Fig. 8. Battery current, voltage, and temperature under nominal scenarios.

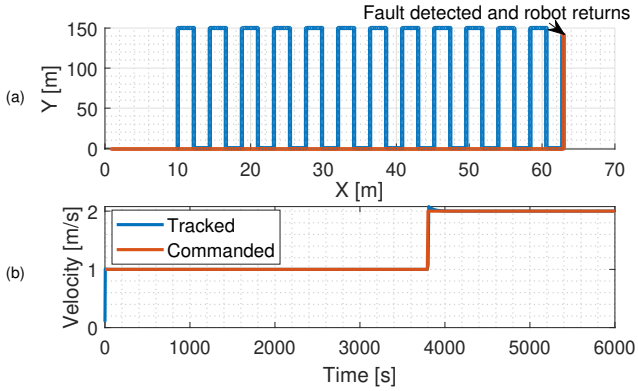

Fig. 9. (a) Trajectory of the robot under battery fault and (b) velocity of the robot under battery fault.

and detection. Again, the closeness of commanded velocity by path planning (in "blue") and actual tracking velocity (in "red") by the robot controller verifies its effectiveness. The battery variables are shown in Fig. 10. As expected, battery current in Fig. 10(a) changed after the fault occurrence and detection when the robot starts returning. The harvesting part shows steady increase in current, again reflecting increase in mass as more and more onions are collected. The temperature response is shown in Fig. 10(c). It can be seen that there is a significant increase in temperature after 4500 s due to the injection of thermal fault induced abnormal heat. Under normal scenario, temperature remained within 300 K while under fault it crossed 310 K – leading to more than 10 K increase. Corresponding response of the temperature residual is shown in Fig. 10(d). At the beginning, the residual starts at non-zero value due to incorrect initialization, but quickly converges to 0 K. After the fault injection around 4500 s, the residual signal changes from 0 K to beyond 0.1 K – indicating a fault occurrence. Accordingly, as mentioned before, the algorithm raised an alarm and the robot started returning to the base. In summary, this study verifies the effectiveness of the algorithmic framework under faulty scenario.

Next, we will briefly compare our proposed framework with some of the most relevant existing approaches [30], [31]. In

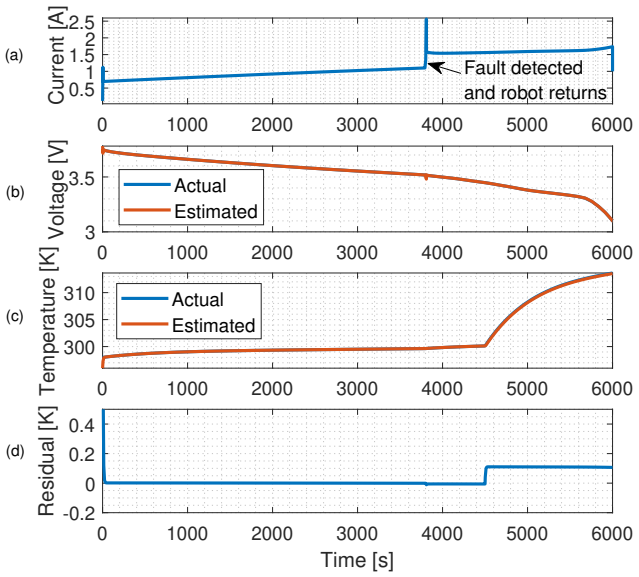

Fig. 10. Battery (a) current, (b) voltage, (c) temperature, and (d) temperature residual under fault.

[31], remaining energy is estimated using the battery voltage-energy curve in an "open-loop" manner and without considering battery internal states. In [31], the remaining battery capacity was tracked using phenomenological approach such as coulomb counting. Such "open-loop" estimation without consideration of internal battery physics can be prone to uncertainties and lead to possibly inaccurate estimates. In our approach, we combined physics-based battery model which captures internal states and coupled it with feedback-based estimator. Use of physics model and feedback can potentially suppress the effect of uncertainties. Finally, none of the aforementioned approaches provided a mechanism to handle battery faults nor they provided any framework for combining mechanism design, path planning, and battery management – which are the key contributions of our work.

IV. CONCLUSIONS

In this work, we have developed an algorithmic framework for energy and safety-awareness of battery-powered autonomous robots in agricultural operation. The specific case study is an onion-harvesting application where the autonomous robot moves and harvests onions. The results indicate the promise of model-based energy- and safety-aware algorithms for autonomous robot operation in agriculture. Despite the promise, it is important to mention some potential limitations of the proposed framework: (i) As the harvestor model parameters heavily depend on soil conditions, the harvestor model developed in this paper may not be readily transferrable to other types of soil conditions; (ii) A shorter path to return the base can be planed through the field that can increase the harvesting time for the robot. (iii) To realize the battery estimation and detection approach, knowledge of battery physical parameters are essential which may require additional experimental characterization. Addressing these limitations should be considered as future work.

REFERENCES

[1] A. Beriya, "Digital agriculture: Challenges and possibilities in india," 2020.

[2] S. Tankha, D. Fernandes, and N. Narayanan, "Overcoming barriers to climate smart agriculture in india," *International Journal of Climate Change Strategies and Management*, vol. 12, no. 1, pp. 108–127, 2020.

[3] T. Mehta and R. Yadav, "Development and performance evaluation of tractor operated onion harvester," *Agric. Mech. Asia Afr. Latin Am.*, vol. 46, no. 4, p. 8, 2015.

[4] http://web.archive.org/web/20080207010024/http://www.808multimedia.com/winnt/kernel.htm.

[5] http://www.topair-usa.com/products.html.

[6] W. LePori and P. Hobgood, "Mechanical harvester for fresh market onions," *Transactions of the ASAE*, vol. 13, no. 4, pp. 517–0519, 1970.

[7] T. Hiroshi, "Onion harvester machine," Jan. 20 1953, uS Patent 2,625,781.

[8] D. Kido and D. Shuff, "Onion harvester with leaf topper," Mar. 7 2006, uS Patent 7,007,449.

[9] S. Hong, K. Lee, Y. Cho, and W. Park, "Development of welsh onion harvester for tractor," *Journal of Biosystems Engineering*, vol. 39, no. 4, pp. 290–298, 2014.

[10] N. Nisha and B. Shridar, "Development of power tiller operated harvester for small onion (allium cepa var. aggregatum)," *International Journal of Agricultural*, vol. 8, no. 1, pp. 73–78, 2018.

[11] M. N. Erokhin, A. S. Dorokhov, A. V. Sibirev, A. G. Aksenov, M. A. Mosyakov, N. V. Sazonov, and M. M. Godyaeva, "Development and Modeling of an Onion Harvester with an Automated Separation System," *AgriEngineering*, vol. 4, no. 2, pp. 380–399, 2022.

[12] L. Kumawat and H. Raheman, "Mechanization in onion harvesting and its performance: A review and a conceptual design of onion harvester from Indian perspective," *Journal of The Institution of Engineers (India): Series A*, pp. 1–10, 2022.

[13] S. Chakraborty, D. Elangovan, P. L. Govindarajan, M. F. ELnaggar, M. M. Alrashed, and S. Kamel, "A comprehensive review of path planning for agricultural ground robots," *Sustainability*, vol. 14, no. 15, 2022. [Online]. Available: https://www.mdpi.com/2071-1050/14/15/9156

[14] L. C. Santos, F. N. Santos, E. J. Solteiro Pires, A. Valente, P. Costa, and S. Magalhães, "Path planning for ground robots in agriculture: a short review," in *2020 IEEE International Conference on Autonomous Robot Systems and Competitions (ICARSC)*, 2020, pp. 61–66.

[15] L. Droukas, Z. Doulgeri, N. L. Tsakiridis, D. Triantafyllou, I. Kleitsiotis, I. Mariolis, D. Giakoumis, D. Tzovaras, D. Kateris, and D. Bochtis, "A Survey of Robotic Harvesting Systems and Enabling Technologies," *Journal of Intelligent Robotic Systems*, vol. 107, no. 2, p. 21, 2023. [Online]. Available: https://doi.org/10.1007/s10846-022-01793-z

[16] A. Basiri, V. Mariani, G. Silano, M. Aatif, L. Iannelli, and L. Glielmo, "A survey on the application of path-planning algorithms for multi-rotor uavs in precision agriculture," *The Journal of Navigation*, vol. 75, no. 2, p. 364–383, 2022.

[17] L. Santos, F. Santos, J. Mendes, P. Costa, J. Lima, R. Reis, and P. Shinde, "Path planning aware of robot's center of mass for steep slope vineyards," *Robotica*, vol. 38, no. 4, p. 684–698, 2020.

[18] D. Bochtis, H. Griepentrog, S. Vougioukas, P. Busato, R. Berruto, and K. Zhou, "Route planning for orchard operations," *Computers and Electronics in Agriculture*, vol. 113, pp. 51–60, 2015. [Online]. Available: https://www.sciencedirect.com/science/article/pii/S0168169914003342

[19] J. Pak, J. Kim, Y. Park, and H. I. Son, "Field evaluation of path-planning algorithms for autonomous mobile robot in smart farms," *IEEE Access*, vol. 10, pp. 60 253–60 266, 2022.

[20] C.-W. Jeon, H.-J. Kim, C. Yun, X. Han, and J. H. Kim, "Design and validation testing of a complete paddy field-coverage path planner for a fully autonomous tillage tractor," *Biosystems Engineering*, vol. 208, pp. 79–97, 2021. [Online]. Available: https://www.sciencedirect.com/science/article/pii/S1537511021001082

[21] Y. Bai, B. Zhang, N. Xu, J. Zhou, J. Shi, and Z. Diao, "Vision-based navigation and guidance for agricultural autonomous vehicles and robots: A review," *Computers and Electronics in Agriculture*, vol. 205, p. 107584, 2023.

[22] L. Wang and M. Liu, "Path Tracking Control for Autonomous Harvesting Robots Based on Improved Double Arc Path Planning Algorithm," *Journal of Intelligent Robotic Systems*, vol. 100, 2020.

[23] S. Sinalkar and B. B. Nair, "Stereo vision-based path planning system for an autonomous harvester," in *Soft Computing and Signal Processing*,

V. S. Reddy, V. K. Prasad, J. Wang, and K. T. V. Reddy, Eds. Singapore: Springer Singapore, 2020, pp. 499–510.

[24] M. Tomy, B. Lacerda, N. Hawes, and J. L. Wyatt, "Battery charge scheduling in long-life autonomous mobile robots via multi-objective decision making under uncertainty," *Robotics and Autonomous Systems*, vol. 133, p. 103629, 2020.

[25] M. Partovibakhsh and G. Liu, "An adaptive unscented kalman filtering approach for online estimation of model parameters and state-of-charge of lithium-ion batteries for autonomous mobile robots," *IEEE Transactions on Control Systems Technology*, vol. 23, no. 1, pp. 357–363, 2014.

[26] F. Zhang, G. Liu, L. Fang, and H. Wang, "Estimation of Battery State of Charge With H-infinity Observer: Applied to a Robot for Inspecting Power Transmission Lines," *IEEE Transactions on Industrial Electronics*, vol. 59, no. 2, pp. 1086–1095, 2011.

[27] A. A. Chellal, J. Lima, J. Gonçalves, and H. Megnafi, "Battery management system for mobile robots based on an extended Kalman filter approch," in *2021 29th Mediterranean Conference on Control and Automation (MED)*. IEEE, 2021, pp. 1131–1136.

[28] L. Jaiem, S. Druon, L. Lapierre, and D. Crestani, "A step toward mobile robots autonomy: energy estimation models," in *Towards Autonomous Robotic Systems: 17th Annual Conference, TAROS 2016, Sheffield, UK, June 26–July 1, 2016, Proceedings 17*. Springer, 2016, pp. 177–188.

[29] V. Berenz, F. Tanaka, and K. Suzuki, "Autonomous battery management for mobile robots based on risk and gain assessment," *Artificial Intelligence Review*, vol. 37, pp. 217–237, 2012.

[30] A. Kottas, A. Drenner, and N. Papanikolopoulos, "Intelligent power management: Promoting power-consciousness in teams of mobile robots," in *2009 IEEE International Conference on Robotics and Automation*. IEEE, 2009, pp. 1140–1145.

[31] F. Dressler and G. Fuchs, "Energy-aware operation and task allocation of autonomous robots," in *Proceedings of the Fifth International Workshop on Robot Motion and Control, 2005. RoMoCo'05.* IEEE, 2005, pp. 163–168.

[32] X. Zeng, L. Burnoski, J. Agui, and A. Wilkinson, "Calculation of excavation force for isru on lunar surface," in *45th AIAA aerospace sciences meeting and exhibit*, 2007, p. 1474.

[33] E. McKyes and O. Ali, "The cutting of soil by narrow blades," *Journal of Terramechanics*, vol. 14, no. 2, pp. 43–58, 1977.

[34] P. Wheeler and R. Godwin, "Soil dynamics of single and multiple tines at speeds up to 20 km/h," *Journal of Agricultural Engineering Research*, vol. 63, no. 3, pp. 243–249, 1996.

[35] V. Tiwari, "Tractor, implement and soil force consideration for tillage implement design, iit kharagpur," July 2018.

[36] J. Tong and B. Z. Moayad, "Effects of rake angle of chisel plough on soil cutting factors and power requirements: A computer simulation," *Soil and Tillage Research*, vol. 88, no. 1-2, pp. 55–64, 2006.

[37] T. K. Khura, I. Mani, and A. Srivastava, "Some engineering properties of onion crop relevant to design of onion digger," *Journal of Agricultural Engineering*, vol. 47, no. 1, pp. 1–8, 2010.

[38] W. Brixius, "Traction prediction equations for bias ply tires," *American Society of Agricultural Engineers (Microfiche collection)(USA)*, 1987.

[39] S. Santhanagopalan and R. E. White, "Online estimation of the state of charge of a lithium ion cell," *Journal of power sources*, vol. 161, no. 2, pp. 1346–1355, 2006.

[40] M. Guo and R. E. White, "Thermal model for lithium ion battery pack with mixed parallel and series configuration," *Journal of the Electrochemical Society*, vol. 158, no. 10, p. A1166, 2011.

[41] S. Dey, B. Ayalew, and P. Pisu, "Nonlinear robust observers for state-of-charge estimation of lithium-ion cells based on a reduced electrochemical model," *IEEE Transactions on Control Systems Technology*, vol. 23, no. 5, pp. 1935–1942, 2015.

[42] S. Al Hallaj, H. Maleki, J.-S. Hong, and J. R. Selman, "Thermal modeling and design considerations of lithium-ion batteries," *Journal of power sources*, vol. 83, no. 1-2, pp. 1–8, 1999.

[43] D. Bernardi, E. Pawlikowski, and J. Newman, "A general energy balance for battery systems," *Journal of the electrochemical society*, vol. 132, no. 1, p. 5, 1985.

[44] R. Firoozi, S. Sattarzadeh, and S. Dey, "Cylindrical battery fault detection under extreme fast charging: A physics-based learning approach," *IEEE Transactions on Energy Conversion*, vol. 37, no. 2, pp. 1241–1250, 2021.